



## Study of the removal efficiency of arsenic from aqueous solutions using *Melia azedarach* sawdust modified with FeO: isotherm and kinetic studies

Mojtaba Davodi<sup>a</sup>, Hossein Alidadi<sup>b</sup>, Azam Ramezani<sup>b</sup>, Farideh Jamali-Behnam<sup>c</sup>, Ziaeddin Bonyadi<sup>b,\*</sup>

<sup>a</sup>Department of Environmental Health, School of Health, Health Sciences Research Center, Torbat Heydariyeh University of Medical Sciences, Torbat Heydariyeh, Iran, email: Davoudi85@gmail.com

<sup>b</sup>Department of Environmental Health Engineering, Social Determinants of Health Research Center, Mashhad University of Medical Sciences, Mashhad, Iran, Tel: +98-5138552610; Fax: +98-5138522775; emails: Bonyadiz@mums.ac.ir (Z. Bonyadi), Alidadih@mums.ac.ir (H. Alidadi), Ramezania912@mums.ac.ir (A. Ramezani)

<sup>c</sup>Department of Environmental Health Engineering, Student Research Committee, School of Health, Mashhad University of Medical Sciences, Mashhad, Iran, email: fjbhnam2009@yahoo.com

Received 4 April 2018; Accepted 28 September 2018

### ABSTRACT

Arsenic (As) is one of the worst toxicants among trace elements, adversely affecting human beings. The removal of arsenic from aqueous solutions was studied using *Melia azedarach* sawdust modified with FeO (MSFeO) as the adsorbent. Arsenic removal was experimentally conducted using MSFeO, based on different parameters including pH (2.77–11.23), time (23.47–171.52 min), the concentration of arsenic (0.04–1.16 mg/L), and adsorbent dose (2.95–17.05 g/L). The characteristics of the synthesized adsorbent were also determined via scanning electron microscope imaging and Fourier-transformed infrared technique. The results indicated that the maximum removal efficiency of As (70.7%) occurred under 0.2 mg/L initial arsenic, 15 g/L adsorbent, pH 4, and contact time of 15 min. The adsorption process was well fitted with the Langmuir model for the majority of samples tested. The experimental data were suitably fitted by the pseudo-second-order kinetic model. The results confirmed that the adsorption rate of arsenic had a direct relationship with the adsorbent dose, contact time, and pH and an inverse relationship with the initial concentration of arsenic.

*Keywords:* Arsenic; *Melia azedarach*; Adsorption; Isotherm; Kinetics

### 1. Introduction

Arsenic (As) is highly resistant against environmental factors. It has adverse effects on the liver, lungs, bladder, and skin. It leads to the increased cardiovascular diseases and hypertension [1]. One of the problems of this pollutant is that it is not degraded into a safe product and hence becomes more concentrated in the recipient organisms because of their bioaccumulation characteristics [2,3]. As is one of the worst toxicants among trace elements, adversely affecting human beings [4]. As(V) and As(III) are the two main forms of

arsenic in aqueous environments [5]. According to the World Health Organization, the maximum permissible level of arsenic is determined to be 10 µg/L in drinking water [6]. Based on investigations, arsenic removal has been studied by various technologies, i.e. ion exchange [7], reverse osmosis [8], adsorption [9], coagulation [10], and photocatalytic oxidation [11]. Among the mentioned methods, adsorption is considered a successful process for arsenic removal from aqueous environments due to its excellent characteristics such as low cost, availability, profitability, ease of operation, and high efficiency [12]. The adsorption of arsenic has been performed by different materials, e.g. activated carbon [13], activated

\* Corresponding author.

alumina [14], biochars modified with Ca and Fe [15], co-modified bentonite with manganese oxides [16], and nonporous geopolymers modified with iron oxide. *Melia azedarach* is frequently found in India, China, Australia, Pakistan, and Iran. *M. azedarach* can be effective in the treatment of environment polluted by tannery effluents [17]. Recently, the modification of adsorbent with iron oxides has increased due to their significant properties including a large area and high affinity toward metal ions [18]. The aim of this study was to examine the removal efficiency of As from aqueous solutions by *Melia azedarach* sawdust modified with FeO (MSFeO) and evaluate the adsorption capacity with different kinetic and isotherm models.

## 2. Materials and methods

### 2.1. Materials

Ferric chloride (FeCl<sub>3</sub>), sodium hydroxide (NaOH), hydrochloric acid (HCl), and arsenic trioxide (As<sub>2</sub>O<sub>3</sub>) were purchased from Merck Company.

### 2.2. Preparation of MS

*Melia azedarach* is a tall deciduous tree belonging to the family Meliaceae. This tree is a fast-growing wild tree and native to Iran. The adult tree has rounded crown and commonly attains a height of 7–12 m. In view of the prevalence of *M. azedarach* in the tropical areas of Iran, the dry leaves and bark of the plant were used to treat arsenic-containing water. It was considered for arsenic removal due to advantages such as low cost, simplicity, and widespread distribution. *Melia azedarach* was obtained from a location near Mashhad city, washed with distilled water (DW), and then dried at 70°C for 24 h. The prepared material was ground to less than 50 meshes, boiled in 10% HCl for 1 h, and ultimately dried at 70°C for 12 h.

### 2.3. Preparation of MSFeO

MSFeO was prepared according to the procedure described as follows: A total of 50 g of the prepared MS was dispersed in 1,000 mL reaction solution containing ferric chloride (0.75M) and hydrochloric acid (3M). After shaking for 4 h, the mixture was allowed to precipitate for 1 h. The supernatant was discharged and the retained material was transferred to an oven and heated at 100°C. After 12 h of heating, in order to remove excessive HCl and FeCl<sub>3</sub> from the surface of the prepared adsorbent, sawdust was washed with distilled water several times over a filter paper (Whatman no. 42). Finally, the prepared adsorbent was dried in the oven at 80°C for another 12 h. To determine the size of the particles, the dried materials were sieved through 50 meshes. The moisture content of 0.7405% was determined for iron oxide-modified sawdust according to the standard method [19].

### 2.4. Characterization

The surface morphology of MSFeO was determined using a scanning electron microscope (SEM) before and after the adsorption of As(III). Fourier-transformed infrared (FTIR) spectroscopy was carried out on pristine and As-loaded

MSFeO using Thermo Nicolet Avatar 370 FTIR ranging from 400 to 4,000/cm.

### 2.5. Preparing the reaction mixtures

As shown in Table 1, for studying the removal efficiency of arsenic, initially, 100 mL of reaction mixture was provided with different parameters including an arsenic concentration of 0.04–1.16 mg/L, an adsorbent dose of 2.95–17.05 mg/L, a pH of 2.77–11.23, and a reaction time of 23.48–171.5 min. The experimental design was carried out based on a central composite design. The studied parameters were considered based on the three levels: high (code +1), low (code -1), and medium (code 0). Moreover, the axial points are shown with codes of + $\alpha$  and - $\alpha$  used to estimate the quadratic terms.

The quadratic model for the variables is presented in Eq. 1:

$$Y = \beta_0 + \sum_{i=1}^k \beta_i x_i + \sum_{i=1}^k \beta_{ii} x_i^2 + \sum_{1 \leq i < j \leq k} \beta_{ij} x_i x_j \quad (1)$$

where  $Y$ ,  $\beta_0$ ,  $\beta_i$ ,  $\beta_{ii}$ ,  $\beta_{ij}$ , and  $x_i$  or  $x_j$  are the predicted response, the constant coefficient, regression coefficients for linear effects, quadratic coefficients, interaction coefficients, and the coded values of the parameters, respectively. The models were fitted using the coefficients  $R^2$  and adjusted  $R^2$  ( $R^2_{adj}$ ) [20].

### 2.6. Kinetic and equilibrium study

The adsorption kinetics were carried out using parameters such as 0.25–0.75 mg/L adsorbent dose and 0.2–1 mg/L arsenic concentration, at pH 4, and contact time 30–150 min. Further, the adsorption isotherm was studied in the following conditions: adsorbent concentration 0.25–0.75 mg/L, arsenic concentration 0.2–1 mg/L, pH 10, and contact time 150 min. The experiments were conducted at a constant agitation speed of 160 rpm and at room temperature. In addition, the effect of adsorbent dose on the adsorption capacity (mg/g) was studied and the value of adsorption capacity was calculated by the reaction kinetic models, i.e. the pseudo-first-order and pseudo-second-order models [21,22].

The pseudo-first-order model is expressed as Eq. (2):

$$\log(q_e - q_t) = \log q_e - \frac{K_1}{2.303} \times t \quad (2)$$

Table 1  
Experimental ranges and levels of independent parameters according to RSM design

Parameters	Symbol	Levels				
		- $\alpha$	-1	0	+1	+ $\alpha$
Concentrations of arsenic (mg/l)	$x_1$	0.04	0.2	0.6	1	1.16
pH	$x_2$	2.77	4	7	10	11.23
Adsorbent dose (g/l)	$x_3$	2.95	5	10	15	17.05
Reaction time (min)	$x_4$	23.47	45	97.5	150	171.52

where  $k_1$  (1/min),  $q_e$  (mg/g), and  $q_t$  (mg/g) are the pseudo-first-order kinetic constant, the amount of adsorbed arsenic per unit mass of MSFeO at equilibrium, and the amount of adsorbed arsenic at any time (min), respectively.

The pseudo-second-order model is described in Eq. (3) :

$$\frac{t}{q_t} = \frac{1}{k_2 q_e^2} + \frac{1}{q_e} \times t \quad (3)$$

where  $k_2$  (g/mg/min) is the rate constant of pseudo-second-order sorption.

The Langmuir and Freundlich equations were used to investigate the adsorption isotherms. The Langmuir isotherm is shown in Eq. (4):

$$\frac{C_e}{q_e} = \frac{1}{q_m} C_e + \frac{1}{K_a q_m} \quad (4)$$

where  $q_e$  (mg/g),  $q_m$ ,  $k_a$  (L/mg), and  $C_e$  (mg/L) are expressed as the adsorption capacity in the equilibrium state, the maximum adsorption capacity, the Langmuir equilibrium constant, and the equilibrium concentration of arsenic, respectively.

The equilibrium factor ( $R_L$ ) is indicated in Eq. (5):

$$R_L = \frac{1}{1 + K_L C_0} \quad (5)$$

where  $R_L$  is an additional parameter related to the Langmuir isotherm model. This value was used for describing adsorption conditions as unfavorable ( $R_L > 1$ ), linear ( $R_L = 1$ ), favorable ( $R_L < 1$ ), or irreversible ( $R_L = 0$ ). The linear form of the Freundlich model is presented in Eq. (6):

$$\ln q_e = \ln K_f + \left(\frac{1}{n}\right) \ln C_e \quad (6)$$

where  $K_f$  and  $n$  reflect Freundlich constants linked to sorption capacity and sorption intensity, respectively [21,22].

### 2.7. Analytical methods

A total of 10 mL of the resulting suspension was withdrawn from each Erlenmeyer flask at given time intervals and then centrifuged at 2,000 rpm. Finally, arsenic in the supernatant was measured by an atomic absorption spectrometry apparatus (Varian, USA) at the wavelength of 193.7 nm.

### 3. Results and discussion

Table 2 provides a summary of the results of the study. According to Table 2, the highest removal rate (77.49%) was obtained at an arsenic concentration of 0.2 mg/L, pH of 10, an adsorbent dose of 15 g/L, and contact time of 150 min. The empirical relationship between the removal efficiency of arsenic and the coded variables is shown in Eq. 7:

$$\text{As removal efficiency (\%)} = 53.07 - 7.77x_1 - 3.82x_2 + 3.96x_3 + 6.65x_4 - 1.93x_1x_4 - 1.5x_2x_3 - 2.76x_2x_4 \quad (7)$$

Table 2

Experimental design and response values at different runs of arsenic removal

RUN	As concentration (mg/L)	pH	Adsorbent dose (g/L)	Contact time (min)	As(III) removal rate (%)
1	0.6	7	10	97.5	52.55
2	0.2	4	15	15	70.70
3	0.2	4	15	45	52.21
4	0.6	7	10	23.47	43.82
5	0.6	7	2.95	97.5	46.91
6	0.6	2.77	10	97.5	47.48
7	1	10	15	45	49.07
8	0.6	7	10	97.5	54.93
9	0.2	4	5	45	41.63
10	0.6	7	10	97.5	56.99
11	1	10	15	15	51.39
12	1	4	5	45	27.87
13	0.04	7	10	97.5	62.57
14	0.6	7	10	97.5	49.88
15	0.6	11.23	10	97.5	58.07
16	1.16	7	10	97.5	42.67
17	0.6	7	10	97.5	47.60
18	0.6	7	17.05	97.5	58.15
19	1	10	5	45	47.08
20	1	4	5	150	41.31
21	0.2	10	5	150	66.17
22	1	10	5	150	49.88
23	0.6	7	10	97.5	53.52
24	0.2	1	5	150	65.80
25	0.6	7	10	171.52	61.73
26	0.2	10	15	150	77.49
27	1	4	15	45	38.75
28	0.2	10	15	45	60.95
29	0.2	10	5	45	56.14
30	1	4	15	150	58.56

where  $x_1$  is the initial arsenic concentration,  $x_2$  denotes the pH of the solution,  $x_3$  shows the adsorbent dose, and  $x_4$  represents contact time. Table 3 presents the results of response surface methodology (RSM) and analysis of variance (ANOVA) for the removal rate of As. The results in Table 3 confirmed that  $R^2$ , adjusted  $R^2$ , and adequate precision were 0.9529, 0.938, and 85.87, respectively.

The quadratic model was the most suitable model for fitting the experimental results with independent parameters. ANOVA was used to determine the significance of the model ( $P$  values  $< 0.05$ ). Overall, the results showed that the model was significant ( $P$  values  $< 0.0001$ ). The quality of the model was assessed by the correlation coefficient value ( $R^2$ ). The relatively high value of  $R^2$  (0.9529) indicates a good agreement between the experimental data and the predicted values. The high value of adjusted  $R^2$  ( $\text{Adj } R^2 = 0.9380$ ) is also indicative of a high significance of the model [23].

Fig. 1 reveals the relationship between the actual and predicted removal of arsenic. The results in Fig. 1 suggested

Table 3  
Results of RSM and ANOVA applied to As removal using MSFeO

Source of variation	Sum of squares	Degree of freedom	Mean square	F value	P value
Model	2,911.88	7	415.98	63.64	<0.0001
$x_1$	1,206.22	1	1,206.22	184.53	<0.0001
$x_2$	291.25	1	291.25	44.55	<0.0001
$x_3$	313.26	1	313.26	47.92	<0.0001
$x_4$	883.50	1	883.50	135.16	<0.0001
$x_1x_4$	59.50	1	59.50	9.10	0.0063
$x_2x_3$	35.94	1	35.94	5.50	0.0285
$x_2x_4$	122.21	1	122.21	18.70	0.0003
Lack of fit	85.87	17	5.05	0.44	0.9087
Pure error	57.94	5	11.59		
Cor total	3,055.69	29			

$R^2 = 0.9529$ , Adj  $R^2 = 0.9380$ , Pred  $R^2 = 0.8987$

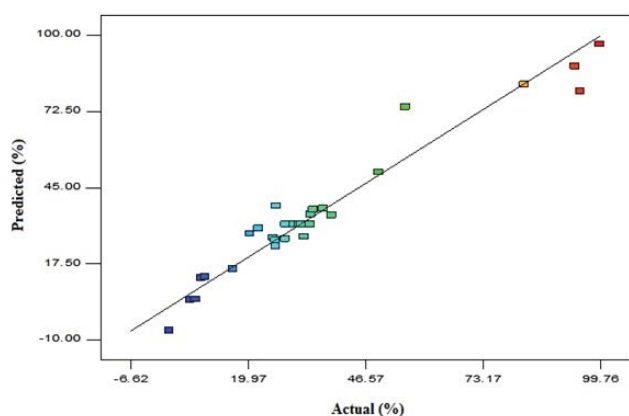


Fig. 1. Actual and predicted removal of arsenic.

that this model is suitable to predict the removal efficiency of arsenic. Accordingly, the predicted arsenic removal rate was 99.76% with the desirability 1. From Eq. (7), the maximum removal efficiency of arsenic was found to be 53.07%, which was affected by different factors. In this equation, the positive sign of the main factors demonstrates their direct effect on the response, whereas the negative sign is related to indirect responses. Hence, it can be concluded that increasing the adsorbent dose and contact time enhances the removal efficiency of arsenic. Further, based on Eq. (7), the initial arsenic concentration with a coefficient of 7.71 was the most important factor influencing arsenic removal.

### 3.1. Effect of independent variables on arsenic removal

#### 3.1.1. Effect of initial arsenic concentration and contact time

Fig. 2 displays the combined effect of contact time and initial arsenic concentration on the As removal. The results in Fig. 2 confirm that there is an inverse relationship between the removal efficiency of arsenic and its initial concentration. This means that with increasing arsenic concentration from 0.2 to 1 mg/L, its removal efficiency decreases by 25.54%. This was due to the affinity between the arsenic molecule

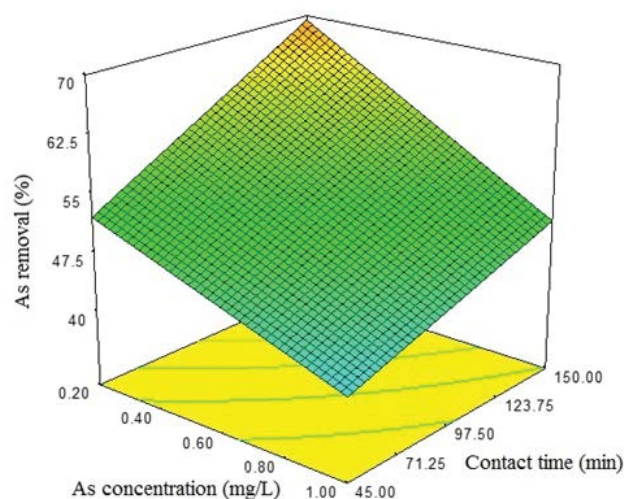


Fig. 2. Combined effect of contact time and initial arsenic concentration on As removal.

and the active sites of MSFeO. On the other hand, with increasing contact time from 45 to 150 min, the removal percentage grew from 46.41% to 59.71%, indicating the faster removal in initial stages of contact time because of the availability of a greater number of free sites for the adsorption [24]. Afterward, the rate of adsorption slowed down due to the decreased free sites on the adsorbent surface [25].

#### 3.1.2. Effect of pH and adsorbent dosage

Fig. 3 indicates the combined effect of pH and adsorbent dosage on the As removal. The results of this study (Fig. 3) suggest that with an increase in the pH from 4 to 10, the removal efficiency of arsenic enhanced from 49.24% to 56.88% ( $P$  value < 0.05). It is necessary to note that when describing the effect of one factor on a response, other variables are fixed at the zero level. For example, when the variable of pH increases from level -1 (4) to +1 (10), the other three variables including concentrations of As (0.2 mg/L), dose of adsorbent (5 g/L), and contact time (45 min) are at the zero

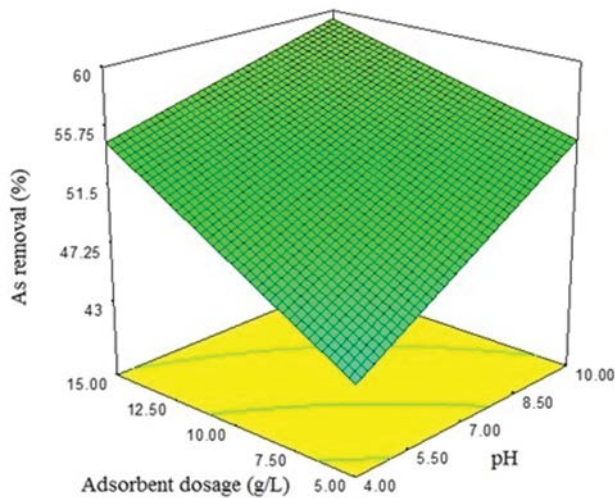


Fig. 3. Combined effect of pH and adsorbent dosage on As removal.

level. In general, the effect of pH on the adsorption process is considerable. This parameter influences aqueous chemistry and surface binding sites of MSFeO [26]. Table 4 summarizes the point of zero charge ( $pH_{pzc}$ ) of MSFeO. The point of zero charge ( $pH_{pzc}$ ) has a great effect on arsenic adsorption, causing the net zero charge on the solid surface of MSFeO. Based on the results of this study (Table 4), pH 4.1 was determined as  $pH_{pzc}$ . At  $pH > pH_{pzc}$ , the electrostatic attraction between arsenic and MSFeO surface increases, which leads to the enhanced As(III) adsorption onto the MSFeO surface. However, at  $pH < pH_{pzc}$ , the surface of MSFeO becomes positively charged resulting in the decreased adsorption of the As(III). Hence, the concentration of the  $H^+$  ions in the solution

Table 4  
Determination of point of zero charge ( $pH_{pzc}$ ) of MSFeO

Initial pH	Final pH
2	2.5
4.2	4.1*
5.5	4
7	4.5
9.5	5.5
11.5	8

\*point of zero charge

Table 5  
Parameters of kinetic model for arsenic adsorption onto MSFeO (pH = 10, arsenic concentration = 0.2 mg/L)

Adsorption dose (g/L)	Pseudo-first-order			Pseudo-second-order		
	$R^2$	$q_e$ (mg/g)	$K_1$ (/min)	$R^2$	$q_e$ (mg/g)	$K_2$ (g/mg/min)
5	0.9447	1.02	0.015	0.9973	0.0096	103.15
10	0.9528	1.08	0.016	0.9969	0.0100	100.01
15	0.9756	0.79	0.015	0.9973	0.0105	95.10

increases, and thus, As(III) adsorption onto MSFeO surface declines with regard to the positive charge of As(III) ions. Saikia et al. indicated that the removal percentage of As(III) was best obtained at pH ranging from 7.5 to 9.5 [27]. Amna et al. confirmed that the maximum As adsorption (93%–98%) was found at slightly alkaline pH 8 [17]. On the other hand, it was found that the removal of arsenic increased gradually with increasing MSFeO dose. Accordingly, with increasing MSFeO dose from 5 to 15 g/L, the removal rate grew from 49.1% to 57.03%. This phenomenon might be due to the high availability of the active sites or surface area at higher doses [28]. Hua revealed that the removal efficiency of arsenic increases by increasing the adsorbent dose within the range of 0–15 mg/L [16].

### 3.2. Adsorption kinetics and isotherms

The parameters of the kinetic model and regression correlation coefficients are presented in Table 5. The results (Table 5) revealed that the adsorption isotherm corresponds with both Langmuir and Freundlich models. For various doses of the adsorbent, the pseudo-second-order model was determined to be the best fitting model, which had the highest determination coefficients ( $R^2 \geq 0.9969$ ) compared with others. Langmuir and Freundlich constants, as well as correlation coefficients, are listed in Table 6. As shown in Table 6, the Langmuir isotherm exhibited the best-fit model ( $R^2 = 0.999$ ) for arsenic removal, compared with the Freundlich model ( $R^2 = 0.983$ ). In addition, the maximum adsorption capacity of MSFeO was obtained to be 0.14 mg/g based on the Langmuir model. Langmuir and Freundlich isotherms describe the mechanism of monolayer sorption with homogenous energy and the mechanism of multilayer sorption with heterogeneous energy, respectively [28,29]. Huang et al. demonstrated that anion resins had exchange capacities of 1.2 mg/g on arsenic [30]. Based on the Freundlich isotherm, the value of  $n$  was obtained to be about 1.6 at an adsorbent dose of 5–15 g/L. Accordingly, the mechanism of adsorption was chemical [31]. Dehghani et al. revealed that the prepared adsorbent had a high adsorption capacity (122.23 mg/g) for As(V) removal [32]. Fazlzadeh et al. showed that Cr(VI) adsorption fitted well with pseudo-second-order kinetic model, and the Langmuir isotherm model was found to describe the adsorption process better [33].

Monda et al. indicated that  $R^2$  values (with pseudo-first-order model) for As concentrations of 10 and 100 mg/L were 0.99 and 0.92, respectively [34]. Maji et al. demonstrated that the  $R^2$  value of the pseudo-second-order model was 0.99 for the arsenic concentration of 0.33 mg/L [35].

Table 6  
Langmuir and Freundlich constants and correlation coefficients

Adsorbent dose (g/L)	Langmuir parameters			Freundlich parameters			
	$Q_0$ (mg/g)	$b$ (L/mg)	$R^2$	$K_f$ (mg/g)	$n$	$R^2$	$R_L$ (dimensionless)
5	0.140	0.226	0.9995	0.160	1.68	0.9838	0.54
10	0.078	0.244	0.9995	0.087	1.67	0.9846	0.55
15	0.056	0.255	0.9983	0.061	1.65	0.9822	0.56

### 3.3. Characterization of the adsorbent

Fig. 4 illustrates the SEM images of MSFeO before and after arsenic adsorption. From Fig. 4(a), the adsorbent surface seems to be rough, with protrusions throughout the micrograph. These can be due to the presence of lignin materials in its structure. The surface roughness is indicative of a high surface area [36]. Taking a glance at Fig. 4(b) reveals surface coverage of the adsorbent after iron oxide coating.

The FTIR analysis was conducted before and after surface modification of sawdust with iron oxide.

Fig. 5 reveals the FTIR analysis before and after arsenic adsorption. Before Fe treatment, there was a broad band at 3,366/cm probably related to the presence of –OH phenolic

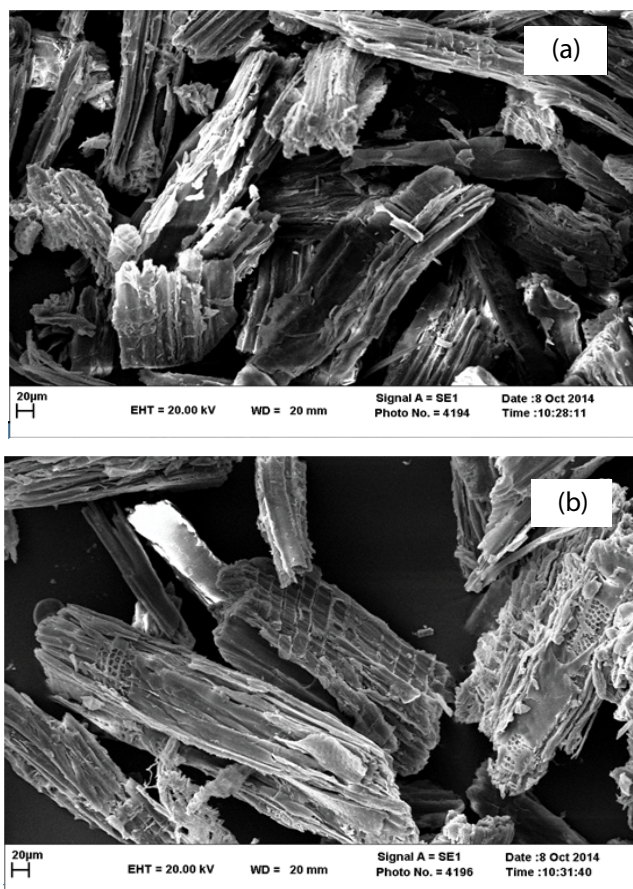


Fig. 4. SEM images of MSFeO (a) before adsorption and (b) after adsorption.

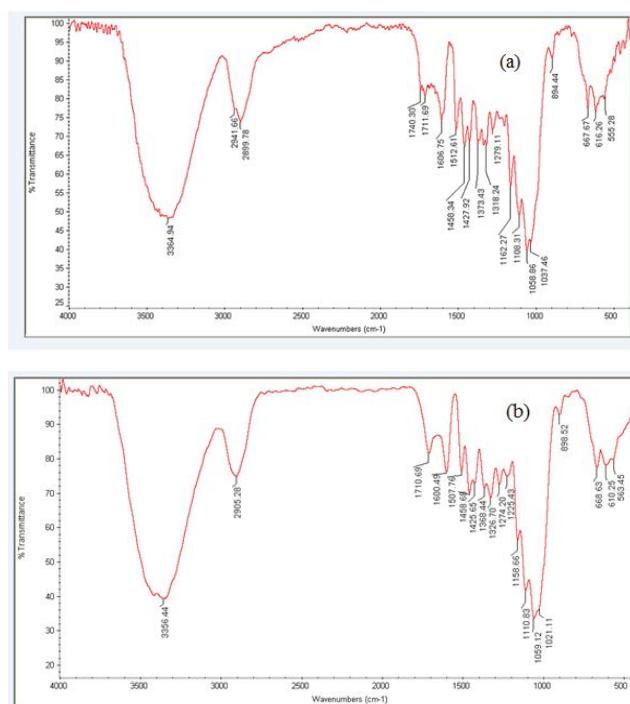


Fig. 5. FTIR spectrum of MSFeO (a) before adsorption and (b) after adsorption.

groups of cellulose and lignin on the surface of the particles. A smaller band at 2,925/cm was likely to indicate the availability of stretching vibration of C–H (methyl and methylene) in aliphatic compounds. The peak at 2,364/cm could be related to N=C functional groups of sawdust according to Chotirat et al. [37] or C=O asymmetric stretching vibration according to Wu and Qiu [38].

The spectrum before iron oxide loading was much different from that after iron oxide coating at lower wave numbers. Numerous peaks appeared in the region below 2,000/cm, indicating the activation of surface sites of sawdust due to Fe loading. The change in this region was also reported by Samsuri et al. in Fe coating of biochars for arsenic removal [39]. The smaller bands at around 500–700/cm might be due to the Fe–O bond vibration of iron oxide deposits [40].

## 4. Conclusion

Based on the obtained results, the effectiveness of sawdust, as a low-cost adsorbent, for arsenite removal could be

greatly enhanced by a coating layer of iron on the surface of the adsorbent. The results indicated that the Langmuir model could suitably explain the adsorption process for the majority of samples tested. The pseudo-second-order kinetic model was the best model to fit the experimental data. The results indicated that the maximum removal efficiency of As (70.7%) occurred at 0.2 mg/L initial arsenic, 15 g/L adsorbent, pH 4, and contact time of 15 min. The results confirmed that the adsorption rate of arsenic had a direct relationship with adsorbent dose, contact time, and pH and an inverse relationship with the initial concentration of arsenic. The results indicated that all the observed bands have had a significant role in the arsenic removal due to the position change of the functional groups based on the FTIR analysis.

## References

- [1] A.A. Duker, E.J.M. Carranza, M. Hale, Arsenic geochemistry and health, *Environ. Int.*, 31 (2005) 631–641.
- [2] S. Khan, Q. Cao, Y.M. Zheng, Y.Z. Huang, Y.G. Zhu, Health risks of heavy metals in contaminated soils and food crops irrigated with wastewater in Beijing, China, *Environ. Pollut.*, 152 (2008) 686–692.
- [3] H. Alidadi, A. Ramezani, M. Davodi, R. Peiravi, P. Maryam, M. Dolatabadi, S. Rafe, Determination of total arsenic in water resources: a case study of Rivash in Kashmar City, *Health Scope*, 4 (2015) e25424.
- [4] T.V. Nguyen, S. Vigneswaran, H.H. Ngo, J. Kandasamy, Arsenic removal by iron oxide coated sponge: experimental performance and mathematical models, *J. Hazard. Mater.*, 182 (2010) 723–729.
- [5] T. Möller, P. Sylvester, D. Shepard, E. Morassi, Arsenic in groundwater in New England—point-of-entry and point-of-use treatment of private wells, *Desalination*, 243 (2009) 293–304.
- [6] S. Maji, Y.H. Kao, C.W. Liu, Arsenic removal from real arsenic-bearing groundwater by adsorption on iron-oxide-coated natural rock (IOCNR), *Desalination*, 280 (2011) 72–79.
- [7] K. Vaaramaa, J. Lehto, Removal of metals and anions from drinking water by ion exchange, *Desalination*, 155 (2003) 157–170.
- [8] R.Y. Ning, Arsenic removal by reverse osmosis, *Desalination*, 143 (2002) 237–241.
- [9] C. Kim, I. Choi, S. Rengara, J. Yi, Arsenic removal using mesoporous alumina prepared via a templating method, *Environ. Sci. Technol.*, 38 (2004) 924–931.
- [10] B.M. Bilici, A. Pala, A statistical experiment design approach for arsenic removal by coagulation process using aluminum sulfate, *Desalination*, 254 (2010) 42–48.
- [11] P.K. Dutta, S. Pehkonen, V.K. Sharma, A.K. Ray, Photocatalytic oxidation of arsenic (III): evidence of hydroxyl radicals, *Environ. Sci. Technol.*, 39 (2005) 1827–1834.
- [12] A. Demirbas, Heavy metal adsorption onto agro-based waste materials: a review, *J. Hazard. Mater.*, 157 (2008) 220–229.
- [13] C. Huang, P. Fu, Treatment of arsenic (V)-containing water by the activated carbon process, *J. Water Pollut. Control Fed.*, 56 (1984) 233–242.
- [14] T.F. Lin, J.K. Wu, Adsorption of arsenite and arsenate within activated alumina grains: equilibrium and kinetics, *Water Res.*, 35 (2001) 2049–2057.
- [15] E.K. Agrafioti, D.E. Dimitrios, Ca and Fe modified biochars as adsorbents of arsenic and chromium in aqueous solutions, *J. Environ. Manage.*, 146 (2014) 444–450.
- [16] J. Hua, Adsorption of low-concentration arsenic from water by co-modified bentonite with manganese oxides and poly (dimethyldiallylammonium chloride), *J. Environ. Chem. Eng.*, 6 (2018) 156–168.
- [17] S. Amna, M. Qaisar, B. Muhammad, A.B. Zulfiqar, P. Arshid, N. Ahmad, R.K. Abdur, S. Sikander, Investigation on Melia azedarach biomass for arsenic remediation from contaminated water, *Desal. Wat. Treat.*, 53 (2015) 1632–1640.
- [18] R. Han, L. Zou, X. Zhao, Y. Xu, F. Xu, Y. Li, Y. Wang, Characterization and properties of iron oxide-coated zeolite as adsorbent for removal of copper(II) from solution in fixed bed column, *Chem. Eng. J.*, 149 (2009) 123–131.
- [19] V. Fierro, G. Muniz, S.G. Gonzalez, M. Ballinas, A. Celzard, Arsenic removal by iron-doped activated carbons prepared by ferric chloride forced hydrolysis, *J. Hazard. Mater.*, 168 (2009) 430–437.
- [20] S. Chatterjee, A. Kumar, S. Basu, S. Dutta, Application of response surface methodology for methylene blue dye removal from aqueous solution using low cost adsorbent, *Chem. Eng. J.*, 181–182 (2012) 289–299.
- [21] Y.S. Ho, G. McKay, The kinetics of sorption of divalent metal ions onto sphagnum moss peat, *Water Res.*, 34 (2000) 735–742.
- [22] Y.S. Ho, Second-order kinetic model for the sorption of cadmium onto tree fern: a comparison of linear and non-linear methods, *Water Res.*, 40 (2006) 119–125.
- [23] M.H. Dehghania, A. Zarei, A. Mesdaghinia, R. Nabizadeh, M. Alimohammadi, M. Afsharnia, Adsorption of Cr(VI) ions from aqueous systems using thermally sodium organobentonite biopolymer composite (TSOBC): response surface methodology, isotherm, kinetic and thermodynamic studies, *Desal. Wat. Treat.*, 85 (2017) 298–312.
- [24] S. Tiantian, A.B. Shams, H. Yunjun, X. Xiaoqin, X. Xinhua, Development, characterization, and evaluation of iron-coated honeycomb briquette cinders for the removal of As (V) from aqueous solutions, *Arab. J. Chem.*, 7 (2014) 27–36.
- [25] S.B. Lalvani, T. Wiltowski, A. Weston, N. Mandich, Removal of hexavalent chromium and metals cations by a novel carbon adsorbent, *Carbon*, 36 (1998) 1219–1269.
- [26] N.W. Wan, M. Hanafiah, Adsorption of copper on rubber (*Hevea brasiliensis*) leaf powder: kinetic, equilibrium and thermodynamic studies, *Biochem. Eng. J.*, 39 (2008) 521–530.
- [27] A. Saikia, B. Saumen, V. Veer, Adsorption isotherm, thermodynamic and kinetic study of arsenic (III) on iron oxide coated granular activated charcoal, *Int. Res. J. Environ. Sci.*, 4 (2015) 64–77.
- [28] M. Rahaman, A. Basu, M. Islam, The removal of As (III) and As (V) from aqueous solutions by waste materials, *Bioresour. Technol.*, 99 (2008) 2815–2823.
- [29] M. Salim, Y. Munekege, Removal of arsenic from aqueous solution using silica ceramic: adsorption kinetics and equilibrium studies, *Int. J. Environ. Res.*, 3 (2009) 13–22.
- [30] J. Huang, F. Nie, F. Peng, Q. Guo, Arsenic removal from wastewater by modified adsorbents, *Proc. Eng.*, 18 (2011) 285–288.
- [31] H.K. Boparai, M. Joseph, D.M. O'Carroll, Kinetics and thermodynamics of cadmium ion removal by adsorption onto nano zerovalent iron particles, *J. Hazard. Mater.*, 186 (2011) 458–465.
- [32] M.H. Dehghani, A. Zarei, A. Mesdaghinia, R. Nabizadeh, M. Alimohammadi, M. Afsharnia, Response surface modeling, isotherm, thermodynamic and optimization study of arsenic (V) removal from aqueous solutions using modified bentonite-chitosan (MBC), *Korean J. Chem. Eng.*, 34 (2017) 757–767.
- [33] M. Fazlzadeh, R. Khosravi, A. Zarei, Green synthesis of zinc oxide nanoparticles using Peganum hamada seed extract, and loaded on Peganum harmala seed powdered activated carbon as new adsorbent for removal of Cr(VI) from aqueous solution, *Ecol. Eng.*, 103 (2017) 180–190.
- [34] P. Monda, C.B. Majumder, B. Mohanty, Effects of adsorbent dose, its particle size and initial arsenic concentration on the removal of arsenic, iron and manganese from simulated ground water by Fe<sup>3+</sup> impregnated activated carbon, *J. Hazard. Mater.*, 150 (2008) 695–702.
- [35] S.K. Maji, A. Pal, T. Pal, Arsenic removal from real-life groundwater by adsorption on laterite soil, *J. Hazard. Mater.*, 151 (2008) 811–820.

- [36] A.S. Mohammadi, M. Sardar, The removal of Penicillin G from aqueous solutions using chestnut shell modified with  $H_2SO_4$ : isotherm and kinetic study, *Iranian J. Health Environ.*, 5 (2013) 497–508.
- [37] L. Chotirat, K. Chaochanchaikul, N. Sombatsompop, On adhesion mechanisms and interfacial strength in acrylonitrile–butadiene–styrene/wood sawdust composites, *Int. J. Adhes. Adhes.*, 27 (2007) 669–678.
- [38] W. Wu, K. Qiu, Vacuum co-pyrolysis of Chinese fir sawdust and waste printed circuit boards. Part I: influence of mass ratio of reactants, *J. Anal. Appl. Pyrolysis*, 105 (2014) 252–261.
- [39] A.W. Samsuri, Z.F. Sadegh, B.B.J. She, Adsorption of As (III) and As (V) by Fe coated biochars and biochars produced from empty fruit bunch and rice husk, *J. Environ. Chem. Eng.*, 1 (2013) 981–988.
- [40] O. Hakami, Y. Zhang, C.J. Banks, Thiol-functionalised mesoporous silica-coated magnetite nanoparticles for high efficiency removal and recovery of Hg from water, *Water Res.*, 46 (2012) 3913–3922.